Orientational order induced by a polymer network in the isotropic phase of liquid crystal

V. Sergan [1,*] T. Sergan,[1] I. Dozov,[2,†] S. Joly,[3,†] and R. Voss[1]

[1]*California State University, Sacramento, 6000 J Street, Sacramento, California 95608, USA*
[2]*PSC, Université de Picardie Jules Verne, 80039 Amiens, France*
[3]*PEDL Laboratory, PSA Technical Center, Route de Gisy, Case courrier VV009, 78943 Vélizy-Villacoublay, France*

We studied the paranematic ordering induced by a polymer network in the isotropic phase of a liquid crystal (LC) that occurs in polymer-stabilized cells with bend configuration of the LC director (π cells) fabricated via photopolymerization of photoreactive monomer RM 82 added in small concentrations (3–5 wt %) to a nematic LC [4-cyano-4′-pentylbiphenyl (5CB)] when low voltage was applied across the cell. The polymer network formed in the nematic phase of the LC consists of fine fibrils that are aligned along the LC director and thus mirror the bend deformation of the LC at the time of polymerization. When heated to temperatures above the nematic-to-isotropic (*N-I*) phase transition such highly ordered polymer network anchors LC molecules providing ordering of the LC around the fibrils which results in unusually high optical retardation of the cell, R_{cell}. We present a theoretical model that relates R_{cell} to the degree of order of the fibrils, the anchoring energy of the LC molecules on the surface of the polymer fibrils, and the fibril radius r_0. Fitting of the experimental $R_{\text{cell}}(T)$ curves with the developed model reveals correlation of r_0 with the nematic correlation length ξ_0 which characterizes penetration of the nematic order in the isotropic phase of the LC. Accepting ξ_0 as a material constant of about 1 nm leads to a very small radius of the fibrils, $r_0 \sim 1$ nm, which is also supported by other reported experimental data. High optical retardation and fast electro-optical response of the cells at the temperatures deep into the isotropic phase point toward the enhancement of the polymer-induced paranematic order by a well-oriented layer of LC molecules that are absorbed on the surface of fibrils. Application of high voltage at the isotropic phase temperatures results in high variations of the optical retardation of the cells. Characteristic on and off response times were about 10–100 μs, independent of the cell gap. Combination of large voltage-driven changes of the optical retardation occurring in the low-viscosity isotropic state with switching times that are at least two orders of magnitude shorter than the typical relaxation times of the cells operating in the nematic phase make such polymer-stabilized π cells very promising for application in fast electro-optical switches and light modulators.

I. INTRODUCTION

Liquid crystals (LCs) confined within a polymer network have been studied extensively due to their applications in electro-optical devices [1]. In these systems the polymer network is usually formed by adding reactive monomers to the LC matrix in various concentrations. Polymerization of the monomers and the formation of the LC-confining polymer network take place under UV light irradiation and, for many applications, in the presence of an external electric field. Adding photopolymerizable monomers to the LC results in segregation of the mixture and formation of LC droplets embedded in the polymer matrix when the polymer concentration is relatively high. These materials are known as polymer-dispersed liquid crystals (PDLCs) [2]. In certain cases, a cellular structure can be formed in which LC is confined in cylindrical cavities [3]. At low monomer concentration (below 5 wt %) the polymer network is composed of highly ordered fibrils that permanently capture the image of the nematic director field [4,5]. Certain types of monomers tend to move to the boundary of the LC layer and form the ordered network in the vicinity of the cell substrates. This happens when polymerization takes place in the presence of an external electric field or when it immediately follows the field application. The resultant morphology of the polymerized layer depends not only on the relative concentration of the monomer in the mixture, but also on its chemical composition and specific conditions during polymerization. Several mechanisms of the segregation were proposed, including the unmixing of low and high molecular weight components due to the Flory-Huggins mechanism [6,7], diaphoresis of polarized LC molecules in electric-field gradients [8,9], geometrical effects in a highly distorted director field [10], and the association of ions with polar groups of the reactive monomers with the subsequent drift of the associates to the electrodes [11].

It is known that in contact with a solid substrate the nematic can retain some orientational order near the boundary even deep in the isotropic phase. This was theoretically described by Sheng [12] and experimentally shown by Miyano [13,14]. The effect is well pronounced in systems with high surface-to-volume ratio, and was observed in PDLCs, LCs confined in

---

*Corresponding author: vsergan@csus.edu

†On leave from Nemoptic, 1 rue Guynemer, F-78114 Magny-les-Hameaux, France.

microporous materials, polymer-stabilized LCs around polymer fibrils, and Aerosil networks [1]. Our interest is the paranematic phase in systems where a low-density ordered polymer network is formed in a uniformly aligned nematic. One of these cases is described in Ref. [4], where the effect of the residual paranematic ordering in the isotropic phase of the polymerized system was quantitatively described for the nematic 5CB doped with 1–4 wt% of diacrylate monomer 4,4′-bis-acryloylbiphenyl (BAB) confined in a capillary tube. Polymerization took place in the presence of a strong electric field that produced a homogeneous director field. Authors detected a weak optical birefringence in the samples deep in the isotropic phase due to the partially ordered polymer network and observed a pretransitional increase of birefringence attributed to the paranematic ordering. They found that the spatial average order parameter for the fibrils is five to eight times smaller than that of the LC environment where it was formed. Strong anchoring parallel to the surface of the fibrils keeps the LC molecules aligned with the polymer within a bundle; however, large spacing between the bundles ($\sim$100 nm) leads to the saturation of the network ordering effect. Separate scanning electron microsopy (SEM) studies of the morphology of the polymer networks in uniformly aligned cells with low concentrations (about 3 wt%) of the BAB-type monomer confirmed that the network was formed of fibrils composed of tightly packed polymer chains [1]. Fibrils were found to be aligned along the LC director forming structures with cylindrical channels parallel to the LC director field capturing it at the time of polymerization. However, direct measurements performed after the LC cell was disassembled and the LC evaporated revealed that the fibril radius and separation distance were different from the ones in cells due to the partial collapse of the structure. In order to find the radius of the fibril, r_0, and the average interfibril distance one has to use a nondestructive method, such as, for example, measuring the optical retardation of the polymerized cell with subsequent modeling.

Surface-induced order in the paranematic phase is best described by applying the Landau–de Gennes formalism. Consider a case when a cylindrical fibril anchors nematic molecules parallel to the surface of the cylinder. In such system the order parameter $S(r)$ of the nematic in the vicinity of the fibril is a decaying function of the distance from the fibril, r. The energy density of the system, f, can be expanded in terms of a single parameter $S(r)$ [4,12,15],

$$f = f_0 + f_1[S(r)] + \frac{L}{2}[\nabla S(r)]^2 + g[S(r) - S_0]^2 \delta(r), \quad (1)$$

where S_o is the surface-preferred value of the nematic order parameter and f_1 is given by

$$f_1 = \frac{a}{2}(T - T^*)S^2(r) - \frac{B}{3}S^3(r) + \frac{C}{4}S^4(r). \quad (2)$$

Here T is the temperature of the system, T^* is the limit of supercooling, and a, B, C, L, and g are phenomenological constants. The last term in (1) is the surface contribution consistent with the Rapini-Papoular surface energy [15].

In the isotropic phase $T > T^*$, and $S(r) \ll 1$ everywhere, and the higher-order terms $S^3(r)$ and $S^4(r)$ in (1) can be neglected. The free energy of the system F is expressed in

the following form,

$$F = \int_V \left(f_0 + f_1[S(r)] + \frac{L}{2}[\nabla S(r)]^2 \right) dV + \frac{1}{2}gA_s[S_0 - S_s]^2, \quad (3)$$

where S_s is the value of the LC order parameter on the surface of the fibril, S_0 is the surface-preferred value of the nematic order parameter that minimizes the surface energy, and A_s is the surface area.

It can be shown that such system is characterized by a temperature-dependent nematic correlation length ξ which describes penetration of the nematic order imposed by polymer fibrils into the bulk of the isotropic phase,

$$\xi = \xi_0 \sqrt{\frac{T^*}{T - T^*}}, \quad (4)$$

where $\xi_0 = \sqrt{\frac{L}{aT^*}} = 0.65$ nm and $T_{N\text{-}I} - T^* \sim 1.1$ K (for 5CB) with $T_{N\text{-}I}$ being the nematic-to-isotropic phase transition temperature [4,12,15]. The model was applied to polymer networks formed from the BAB-type monomers added in concentration of about 3 wt % to nematics [1,4]. Two independent groups reported the radius of the polymer fibrils of about 2 nm (Crawford *et al.* [4]) and 0.5 nm (chapter by Yang *et al.* in [1]), respectively.

Amimori and coauthors [15] pointed out that the continuum approach does not always describe experimental results. They modified the theory by assuming that the order parameter is constant within a thin layer around the fibril and falls exponentially with the increasing distance away from this layer. They applied this model to the nematic 5CB confined in elliptical droplets and found that the experimental results correlated with the Landau–de Gennes theory for $L = 1.7 \times 10^{-11}$ J/m and $a = 0.1319 \times 10^6$ J/(m^3 K) (same as in Refs. [12,16]), whereas T^* and the thickness of the interfacial surface layer depended on the ellipticity of the droplets.

A different approach to modeling was employed by Kraig *et al.* in Ref. [17] where the authors studied birefringence effects in a homogeneous cell with a network of fibrils formed in the absence of applied voltage and aligned parallel to the LC director. In their model, the order parameter spatially varied due to the aligning effect of fibrils [17,18]. Such model was shown to be useful for analysis of pretransitional behavior of such systems [17,18].

To avoid simplifications, without which the problem cannot be solved analytically, computer simulations of paranematic ordering were performed using the Lebwohl-Lasher lattice model [19,20]. In this model the molecular interaction energy is proportional to $\varepsilon[\frac{3}{2}(\hat{u}_i \cdot \hat{u}_j)^2 - \frac{1}{2}]$, where $\hat{u}_i$ and $\hat{u}_j$ are unit vectors corresponding to the orientation of neighboring nematic molecules and ε is related to the reduced temperature as $T_{\text{reduced}} = kT/\varepsilon$, with $T_{\text{reduced}} = 1.0$ deep in the nematic phase and $T_{\text{reduced}} = 1.2$ deep in the isotropic phase [20,21]. Spatial distribution of the order parameter was calculated in assumption of strong anchoring provided by polymer fibrils at the temperatures deep in the nematic as well as isotropic phases. It was found that when the LC molecules are aligned parallel to the fibrils, the degree of order in the isotropic phase decays to zero within a characteristic length comparable to the radius of the polymer fibril.

FIG. 1. π-cell configuration.

FIG. 2. Schematic representation of the structure of polymerized π-cells: lateral (a) and longitudinal (b) cross sections. Polymer chains (represented by solid lines) follow the π-bend configuration of the LC director at the time of polymerization (a). Polymer fibrils with the average radius r_0 are uniformly distributed in the cell at the average half-distance D_0 (b).
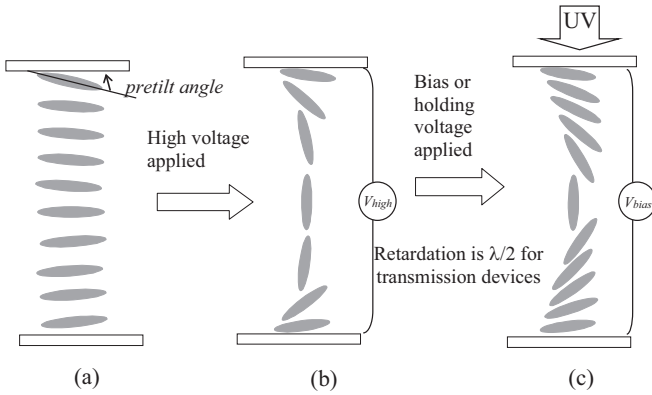
Molecular structures stabilized by polymer networks were extensively studied for applications to electro-optical devices [22,23], for example, for stabilization of π-bend structures in the cells with parallel rub directions (π-cells) [24], Fig. 1. When no voltage is applied to such a cell it is in the splay director configuration (a). Application of high voltage of 10–20 V induces transition to a bend state (b). The cell then can be efficiently switched between the high- (c) and low-retardation state (b) within the same π-bend configuration. Removal of voltage induces the reversal to the splay state via nucleation of domains resulting in deterioration of the optical performance. This transition can be prevented by locking the cell in the bend configuration with the help of a polymer network formed from a photopolymerizable monomer that has chemical properties similar to the LC [24,25].

The localization of the network depends on the chemical composition of the monomer. The available reactive monomers consist of the biphenylene cores with the diacrylate reactive groups directly linked to it [RM 82 and RM 84 (BAB), both by Merck] or cores made of phenyls separated by ester groups (RM 257, also by Merck). In our previous work we found that two types of monomers, RM 84 [26] and RM 257 [27], form a polymer network predominantly at the LC layer boundaries [28–30], whereas RM 82 forms a network in the bulk. The localization of the network also depends on whether the polymerization takes place in the presence of the electric field or immediately follows its application. The association of ions that are inherently present in the LC with the polar groups of the reactive monomers and the subsequent drift of the associates to the electrodes explains the resultant morphology of the system [11]. However, the manipulation of the network localization is difficult due to multiple competing mechanisms of fluid segregation taking place during polymerization. Such systems demonstrate a high degree of ordering resulting in residual birefringence effects when the samples are heated beyond the nematic-to-isotropic (N-I) phase transition.

In this work we investigate such systems and present a two-dimensional theoretical model that relates the paranematic order induced by the polymer network and the resulting optical retardation of the cell, R_{cell}, with the degree of ordering, anchoring energy, and radius of the polymer fibrils, r_0. We show that the observed high value of the optical retardation and the cell's strong and fast response under the electric-field
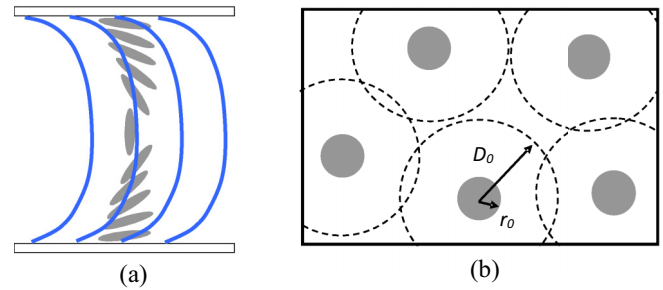
application are due to the small radius of the fibrils and the efficient anchoring of the LC molecules resulting in the formation of a thin and well-oriented LC layer around each fibril. We also discuss the potential of the observed electro-optic effect for practical applications of the polymer-stabilized π-cells in their isotropic state.

II. THEORETICAL MODEL

A. Spatial variation of the order parameter

The orientational order of the nematic can be described by using a unit vector $\hat{n}_\alpha$ that points in the direction of the average orientation of LC molecules, and a scalar order parameter S, which is a function of an average angle between the director and molecular axis. Free energy density of the system, in general, can be described by using a tensor order parameter $Q_{\alpha\beta} = \frac{S}{2}(3\hat{n}_\alpha\hat{n}_\beta - \delta_{\alpha\beta})$ and its first differentials [12]. Molecules of the photoreactive monomer used in our work are chemically similar to LC and thus align along the LC director. During polymerization that takes place at the nematic phase temperatures in the presence of the external electric-field polymer chains are formed parallel to the local director keeping approximately the same degree of order as the LC : $S_{\text{polymer}} \approx S_{\text{LC}}$. Consequently, the axes of the polymer fibrils follow the local director distribution at the time of polymerization memorizing the bend state of the π-cell [Fig. 2(a)].

The SEM pictures of the polymer networks in polymerized cells [1] show that the polymer fibrils are cylindrical in shape, and have relatively small cross-section radii. In this work we study the paranematic order induced by such fibrils in the isotropic phase of LC. Our model assumes that all the monomer in the mixture is polymerized, and that the polymer chains are bundled in fibrils of the same radius r_0. The fibrils are uniformly distributed in the bulk of the LC matrix at the average half-distance D_0 [see Fig. 2(b)]. Geometrically, the ratio r_0/D_0 corresponds to the volume fraction of the monomer in LC, $c : (r_0/D_0)^2 = c$. Due to similar densities, the volume fraction of the monomer approximately equals its mass fraction in LC and its concentration in wt%, thus we will further use c in % rather than wt% throughout of the remainder of the text.

Similarly to the alignment of LCs by polymer alignment layers [31], LC molecules adjacent to the fibrils are anchored to their surfaces resulting in a small but finite paranematic orientational order of LC. In our model we assume that the scalar order parameter of the LC around the fibril has a cylindrical symmetry: $S = S(r)$, where r is the distance from the axis of the fibril. At the temperatures above the *N-I* phase transition the energy density in the bulk of the LC is

$$f_{\text{bulk}} = \frac{1}{2}\left[AS^2 + L\left(\frac{dS}{dr}\right)^2\right].\tag{5}$$

In our model we neglect the higher-order terms because the scalar order parameter in the isotropic phase S is small; $S \ll 1$. The energy per unit length is

$$F_{\text{total}} = 2\pi \int_{r_0}^{D_0} f_{\text{bulk}} r\, dr + 2\pi r_0 W_S(S_s),\tag{6}$$

where $W_S(S_s)$ is the anchoring energy of the LC molecules on the surface of the polymer fibril given by $W_S(S_s) = \frac{1}{2}W(S_0 - S_s)^2$, where S_0 is the order parameter preferred by the surface of the polymer fibril (i.e., the surface order parameter imposed by the fibril in the case of infinitely large anchoring strength), and $S_s = S(r_0)$ is the equilibrium order parameter that minimizes the anchoring energy in the case of finite W. In our model we also assume that $S_0 \approx S_{\text{polymer}}$, where S_{polymer} is the order parameter of the polymer chains. The coefficient W can be estimated from the Rapini-Papoular surface energy $F_s = \frac{1}{2}W_{R-P}\sin^2(\theta_s - \theta_o)$ [32], where θ_o is the pretilt angle imposed by the aligning surface (measured with respect to the interface), and θ_s is the actual molecular tilt angle at the surface. The relationship between W_{R-P} (T) (measured in the nematic phase at a given temperature T), the nematic order parameter on the aligning surface $S_s(T)$ (also measured at the same temperature T), and the temperature-independent coefficient W has been given by Nobili and Durand [33],

$$W = \frac{2W_{R-P}(T)}{9 S_0 S_s(T)}.\tag{7}$$

The minimization of the free energy (6) leads to the Euler-Lagrange equation for $S(r)$,

$$\frac{d^2S}{dr^2} + \frac{1}{r}\frac{dS}{dr} - \frac{1}{\xi^2}S = 0,\tag{8}$$

where $\xi = \sqrt{L/A}$ is the nematic correlation length. Introducing $\rho = r/\xi$ one obtains

$$\rho^2\frac{d^2S}{d\rho^2} + \rho\frac{dS}{d\rho} - \rho^2 S = 0.\tag{9}$$

This equation has a general solution,

$$S(\rho) = \alpha K_0(\rho) + \beta I_0(\rho),\tag{10}$$

where K_0 and I_0 are the modified Bessel functions [34].

At the surface of the fibril the LC order parameter is set at S_s resulting in the boundary condition $S(r_0) = S_s$, and far from the polymer fibril it obeys free boundary conditions $\frac{dS}{dr}|_{r=D_0} = 0$ (see Fig. 3). Application of these boundary conditions
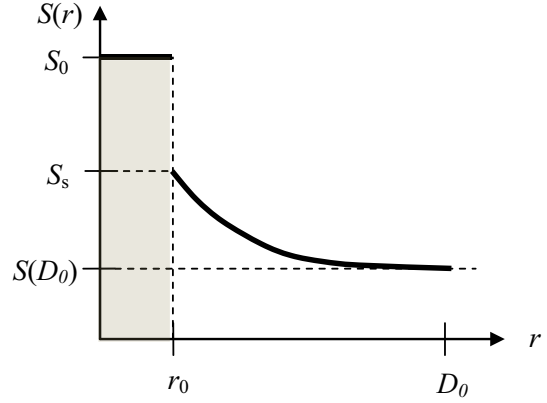
FIG. 3. The order parameter of LC inside the fibril S_0 is approximately equal to the order parameter of the polymer chains S_{polymer} (set during polymerization in the presence of an external electric field in the nematic phase of the LC). S_s is the order parameter in the isotropic phase of the LC induced by the surfaces of fibrils due to the anchoring of the LC molecules to the fibrils.

results in α and β given by the following expressions:

$$\alpha = \frac{I_1(D_0/\xi)}{K_0(r_0/\xi)I_1(D_0/\xi) + K_1(D_0/\xi)I_0(r_0/\xi)}S_s,$$

$$\beta = \alpha\frac{K_1(D_0/\xi)}{I_1(D_0/\xi)} \ll \alpha.\tag{11}$$

The energy per unit length is

$$\begin{aligned}
F_{\text{total}} &= \pi \int_{r_0}^{D_0}\left[AS^2 + L\left(\frac{dS}{dr}\right)^2\right]r\,dr + 2\pi r_0 W_S(S_s)\\
&= \pi L \int_{r_0/\xi}^{D_0/\xi}([\alpha K_0(\rho) + \beta I_0(\rho)]^2\\
&\quad + [-\alpha K_1(\rho) + \beta I_1(\rho)]^2)\rho\,d\rho + \pi r_0 W(S_0 - S_s)^2
\end{aligned}\tag{12}$$

Using the integral formulas for the modified Bessel functions [35] and substituting the constants α and β, we obtain the total energy as a function of the equilibrium value of the order parameter on the surface of the polymer fibril, S_s:

$$F_{\text{total}} = \pi S_s^2 C_2 + \pi r_0 W(S_0 - S_s)^2.\tag{13}$$

Here we introduced the notation $C_2 = C_2(r_0, D_0, \xi) = L\frac{r_0}{\xi}\left[\frac{K_1(r_0/\xi)I_1(D_0/\xi) - K_1(D_0/\xi)I_1(r_0/\xi)}{K_0(r_0/\xi)I_1(D_0/\xi) + K_1(D_0/\xi)I_0(r_0/\xi)}\right]$.

The minimization of the energy with respect to S_s gives

$$S_s = S_0 \bigg/ \left(1 + \frac{C_2}{Wr_0}\right).\tag{14}$$

Equations (11) and (12) completely define the $S(r)$ function in a closed form resulting in its expression through the modified Bessel's functions of integer order.

In the case of the low density of the polymer network $D_0 \gg \xi_0$, the $S(r)$ function simplifies to

$$S(r) = \frac{K_0\left(\frac{r}{\xi}\right)}{K_0\left(\frac{r_0}{\xi}\right)}S_s, \quad S_s = S_0 \bigg/ \left(1 + \frac{C_1}{Wr_0}\right),\tag{15}$$

where

$$C_1 = \frac{Lr_0}{\xi} \frac{K_1(r_0/\xi)}{K_0(r_0/\xi)}; \qquad (16)$$

i.e., $C_2 \to C_1$ when $D_0/\xi_0 \to \infty$.

B. Optical retardation of the cell

Order parameter cannot be measured directly: The measurable quantity in most cases is the optical retardation of the cell. It can be measured easily and precisely as a function of temperature under a polarizing microscope equipped with a heating stage and Berek compensator. The optical anisotropy of the LC-polymer system is defined as $\Delta n = n_\| - n_\perp$, where $n_\|$ and $n_\perp$ are, respectively, the refractive indices for the light polarized parallel and perpendicular to the axis of the fibril. Optical anisotropy varies rapidly inside the sample on the length scale of D_0. Inside the polymer fibril, it is given by $\Delta n_{\mathrm{polymer}} = \Delta n^0_{\mathrm{polymer}} S_{\mathrm{polymer}}$, where S_{polymer} is the order parameter of the polymer chains, and $\Delta n^0_{\mathrm{polymer}}$ is the optical anisotropy of the polymer when $S_{\mathrm{polymer}} = 1$. Outside the fibril, the optical anisotropy of the LC is given by $\Delta n_{\mathrm{LC}} = \Delta n^0_{\mathrm{LC}} S(r)$, where Δn^0_{LC} is the optical anisotropy of the completely ordered nematic, and $S(r)$ is the order parameter induced by the polymer network in the isotropic phase of the LC. As the birefringence varies on a scale much smaller than the wavelength of light, the system behaves optically as a uniform medium with the average optical anisotropy $\overline{\Delta n}$,

$$\overline{\Delta n} = \frac{2}{D_0^2} \left[\int_0^{r_0} \Delta n_{\mathrm{polymer}} r dr + \int_{r_0}^{D_0} \Delta n_{\mathrm{LC}} r dr \right]$$

$$= c S_{\mathrm{polymer}} \Delta n^0_{\mathrm{polymer}} + \langle S_{LC} \rangle \Delta n^0_{\mathrm{LC}}$$

$$= \overline{\Delta n}_{\mathrm{polymer}} + \overline{\Delta n}_{\mathrm{LC}}, \qquad (17)$$

where c is the volume fraction of the polymer in the LC matrix, and $\overline{\Delta n}_{\mathrm{polymer}}$ and $\overline{\Delta n}_{\mathrm{LC}}$ are the respective contributions of the polymer and the LC to the resultant optical anisotropy of the system. $\langle S_{\mathrm{LC}} \rangle = \frac{2}{D_0^2} \int_{r_0}^{D_0} S(r) r dr$ is the average order parameter induced by the polymer fibrils in the isotropic phase of the LC. By using the integral properties of the modified Bessel functions [35] we obtain

$$\langle S_{\mathrm{LC}} \rangle = 2 \frac{\xi^2}{L D_0^2} \frac{S_0}{\frac{1}{C_2} + \frac{1}{r_0 W}} = 2c \frac{\xi^2}{L r_0} \frac{S_0}{\frac{r_0}{C_2} + \frac{1}{W}}, \qquad (18)$$

The order parameter S_{polymer} is expected to be close to the nematic order parameter during polymerization, S_{LC}, typically about 0.65 (at room temperature) [4]. After polymerization, S_{polymer} remains constant and temperature independent due to the stiff structure of the polymerized bundles even at temperatures much higher than the N-I phase transition. For a completely ordered 5CB, when $S = 1$, its optical anisotropy is $\Delta n^0_{\mathrm{LC}} \approx 0.35$, and the average refractive index is $n^{\mathrm{LC}}_{\mathrm{ave}} = (n^{\mathrm{LC}}_\| + 2n^{\mathrm{LC}}_\perp)/3 \approx 1.62$ [4]. Because the molecules of the photopolymerizable monomer are chemically similar to those of 5CB, $\Delta n^0_{\mathrm{polymer}} \approx \Delta n^0_{\mathrm{LC}}$ and $n^{polymer}_{\mathrm{ave}} \approx n^{\mathrm{LC}}_{\mathrm{ave}}$. Using these values in Eqs. (14) and (15), one can obtain the average optical anisotropy $\overline{\Delta n}$ and the average refractive indices, $\overline{n_\|} = \overline{n_{\mathrm{ave}}} + 2\overline{\Delta n}/3$ and $\overline{n_\perp} = \overline{n_{\mathrm{ave}}} - \overline{\Delta n}/3$, as a function of r_0 and ξ. We note that due to a small value of the induced order parameter

$\langle S_{\mathrm{LC}} \rangle$ and low density of the polymer network, $\overline{\Delta n} \ll \overline{n_{\mathrm{ave}}}$ in the isotropic phase.

When the network is formed in the nematic phase in the presence of an external electric field, the fibrils follow the LC director distribution. The director field in the π-bend state is characterized by a tilt angle ϕ_{LC} (measured with respect to the cell substrates) that changes with distance z from the cell substrate. The axes of the fibrils follow the director configuration of LC and thus are also tilted. In our model we assume that the tilt angle for the fibrils is the same as the local tilt of the LC director: $\phi(z) = \phi_{\mathrm{LC}}(z)$. The latter can be calculated via minimization of the free energy of the nematic cell in the presence of the external field. Then the optical retardation of the cell for the light incident normally to the cell substrates is

$$R_{\mathrm{cell}} = \overline{n_\perp} \int_0^d \left(\frac{\overline{n_\|}}{\sqrt{\overline{n_\|}^2 \sin^2\phi + \overline{n_\perp}^2 \cos^2\phi}} - 1 \right) dz$$

$$\approx \overline{\Delta n} \int_0^d \cos^2\phi \, dz = R_{\mathrm{LC}} + R_{\mathrm{residual}}, \qquad (19)$$

where d is the cell thickness. The smallness of the optical anisotropy of LC in the isotropic phase allowed simplification [see Eq. (19)]. Introducing $C_\phi = \frac{1}{d} \int_0^d \cos^2\phi \, dz = \langle \cos^2\phi \rangle$ one can separate the temperature-dependent contribution $R_{\mathrm{LC}} \approx C_\phi d \overline{\Delta n_{\mathrm{LC}}}$, which is due to the polymer-induced paranematic order in the isotropic phase, and the temperature-independent residual retardation $R_{\mathrm{residual}} \approx C_\phi d \overline{\Delta n_{\mathrm{polymer}}}$, which is due to the ordered polymer network. Thus, the optical retardation of the cells measured experimentally at different temperatures above the N-I phase transition can be fitted by using two primary fitting parameters, r_0 and ξ_0. The anchoring strength coefficient W was estimated according to Eq. (7) from $W_{R\text{-}P}$ in the Rapini-Papoular anchoring energy that was measured for the RM 82-5CB interface in our previous work [31]. Measurements were performed by using the technique proposed in Refs. [36,37]; the required values of the pretilt angle were measured as in Ref. [38].

III. EXPERIMENT

A. Cell fabrication and measurement of the optical retardation vs temperature

To investigate the paranematic state induced by the ordered polymer network, we fabricated a series of polymer-stabilized π-cells by polymerizing a photoreactive monomer added in small concentrations to nematic LC. Polymerization took place in the presence of an external electric field that induced a π-bend director configuration [Fig. 1(c)]. The bend state was considered stable and the polymer network uniformly distributed within the bulk of the LC if the cells did not overcome the bend-to-splay transition after the removal of the applied voltage. Concentrations of the monomer below 3 % did not result in a stable bend state, whereas cells with concentrations above 5 % demonstrated high light scattering and thus were not used in this work. We found [28] that polymerization conditions, such as temperature, power density, and the wavelength of UV light, as well as the duration of exposure, greatly influence the final structure of the polymer network resulting in the networks spreading through the bulk of the

cell or being localized in the vicinity of the cell substrates. We selected the materials and identified the conditions for which the polymer network uniformly permeated the whole cell, efficiently stabilized the bend state, produced low light scattering, and induced high paranematic order in the isotropic phase of the LC. These properties indicate that the networks were composed of fine and well-oriented fibrils that efficiently anchored LC molecules.

π-cells with the cell gaps of $d = 4.3$ and 5.3 microns were fabricated by using a glass substrates with an indium-tin oxide conducting layer covered with rubbed polyimide PI 2555 (by DuPont) that served as an alignment layer for the LC. The cell gap was controlled by spacers in the gasket. The cells were assembled with rub directions being parallel, which provided for the π-bend director configuration at low applied voltage. They were filled with a mixture of the RM 82 monomer (by Merck), 5CB, and a photoinitiator. The cells were polymerized at 2.4 V ac (1–3 kHz) applied across the cell by using a UV light source with a power density of 1–50 mW/cm^2 in both the UVA and UVB spectra for about 40 min.

The head-on optical retardation of the cells was measured as a function of temperature T in the nematic and isotropic phases under a polarizing microscope equipped with a Berek compensator. The temperature of the cells was controlled by a MK-1 temperature controller (by Instec). For the time-dependent and for high-precision steady-state birefringence measurements we used a microphotometer (D-104, PTI) mounted on a Leitz Ortholux polarizing microscope that was equipped with a photomultiplier tube (PMT). The load resistance on the PMT anode was chosen to be small, about 1 kΩ, which ensured its fast response and gave a capability of measurement of characteristic times in the submicrosecond range. The voltage drop on the load resistor was accumulated for up to 512 counts and measured by using a digital oscilloscope (TDS 3014, Tektronix). The resolution of the optical path difference measured with this setup was better than 0.3 nm for the steady-state measurements and better than 0.05 nm for the time-dependent studies when short pulses of sinusoidal ac voltage were applied across the cell.

Figure 4 shows the measured optical retardation $R_{cell}(T)$ curves for a 4.3-microns-thick π-cells filled with the mixture of 5CB and 3%, 4%, and 5% RM 82 and polymerized at the applied voltage of 2.4 V. The π-bend configuration achieved in these three cells was stable in the absence of the electric field. A 5.3-μm-thick cell filled with the mixture of 5CB and 3.5% RM 82 was fabricated at the same conditions. This cell reverted to splay configuration after it was polymerized, however, a stable bend configuration in the nematic phase was restored after the repeated application of high voltage at the isotropic phase temperatures.

The *N-I* phase transition in the polymerized cells occurs at $T_{N-I} = 33\,^{\circ}\text{C}$–$34\,^{\circ}\text{C}$, which is lower than for pure 5CB ($T_{N-I} = 35.1\,^{\circ}\text{C}$). The optical retardation of the cells R_{cell} decreases as temperature increases but its value remains high, about 30–80 nm, at the temperatures close to T_{N-I}. It decreases further as temperature increases but remains non-negligible even far from the *N-I* transition. It asymptotically converges to a constant value $R_{residual}$, the residual retardation due to the ordered polymer network, at $T \sim 80\,^{\circ}\text{C} - 100\,^{\circ}\text{C}$.
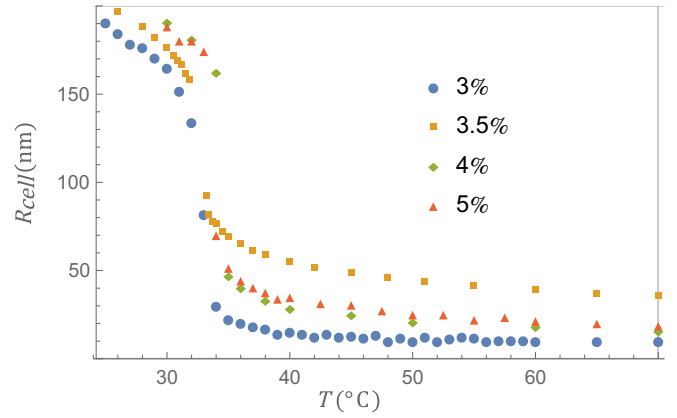
FIG. 4. $R_{cell}(T)$ curves for 4.3-μm-thick cell filled with the mixture of 5CB and 3%, 4%, and 5% of RM 82, respectively, and a 5.3-μm-thick cell filled with the mixture of 5CB and 3.5% of RM 82; all are polymerized at 2.4 V.

B. Curve fitting procedure

Modeling of $R_{cell}(T)$ curves was performed in two steps. First, the curves were fitted assuming no interaction between the polymer fibrils by using the relationship

$$R_{cell} = \frac{2c\sigma S_0}{\frac{r_0}{\xi} \frac{K_0(r_0/\xi)}{K_1(r_0/\xi)} + \frac{L r_0}{W\xi^2}} + R_{iso}, \qquad (20)$$

where R_{iso} was the residual retardation of the cell deep in the isotropic phase taken from experiment, $\xi = \xi_0 \sqrt{\frac{T^*}{T - T^*}}$, $W = \frac{2W_{R-P}}{9S_0^2}$, and σ was the optical retardation of the π cell calculated from the LC director distribution corresponding to the applied voltage of 2.4 V. Calculations of the LC director's tilt angle for the π-cell at the nematic phase temperatures was performed by minimizing the free energy of the cell in the bend state in the presence of the external electric field [director configuration is shown in Figs. 1(b) and 1(c)]. The Euler-Lagrange formalism was used to obtain the equation of motion for the director polar angle $\phi_{LC}(z)$, and then the standard relaxation technique was used to solve it numerically. The LC cell was divided into sublayers, and the angle ϕ_{LC} in each sublayer was calculated numerically. Due to strong anchoring of LC molecules by the cell's alignment layers, the pretilt angle at the LC boundaries [Fig. 1(a)] was kept constant for all applied voltages. Calculations were performed by using TCO 7.2 software [39].

After the preliminary values of T^*, ξ, and r_0 were found in the first round of modeling, the same experimental curves were fitted by using Eq. (21),

$$R_{cell} = \frac{2c\sigma S_0}{\left[\frac{K_o\left(\frac{r_0}{\xi}\right) I_1\left(\frac{D_0}{\xi}\right) + I_0\left(\frac{r_0}{\xi}\right) K_1\left(\frac{D_0}{\xi}\right)}{K_1\left(\frac{r_0}{\xi}\right) I_1\left(\frac{D_0}{\xi}\right) - I_1\left(\frac{r_0}{\xi}\right) K_1\left(\frac{D_0}{\xi}\right)}\right] \frac{r_0}{\xi} + \frac{L r_0}{W\xi^2}} + R_{iso}, \quad (21)$$

that was derived in assumption of a finite half-distance between fibrils D_0, and the additional condition on D_0 given by Eq. (22),

$$D_0 = \frac{r_0}{\sqrt{c}}. \qquad (22)$$

TABLE I. Fitting parameters that produce a satisfactory fit of $R_{\text{cell}}(T)$ curve for the cell filled with 3% RM 82. In all cases D_0 correlated to r_0 as $D_0 = r_0/\sqrt{c}$.

r_0	ξ_0	T^*
1 nm	1 nm	306 K
5 nm	3.2 nm	304.5 K
10 nm	5 nm	304.5 K
50 nm	11 nm	304.5 K
100 nm	17 nm	304.5 K
100 nm	80 nm	306 K

In all cases we used the following material parameters: $n_\perp^{\text{LC}} = 1.5$, $\Delta n_{\text{LC}}^0 = 0.35$ [4], $S_0 = 0.65$ [4], and $W_{R\text{-}P} = 2 \times 10^{-4}$ J/m^2 [31]. In our experiment, the retardation of the π-cells at the temperatures deep in the isotropic phase was very close to the factor of $c\sigma S_0$. Thus, we also explored the applicability of the following relationship:

$$R_{\text{cell}} = \frac{2R_{\text{iso}}}{\left[\frac{K_o\left(\frac{r_0}{\xi}\right)I_1\left(\frac{D_0}{\xi}\right)+I_0\left(\frac{r_0}{\xi}\right)K_1\left(\frac{D_0}{\xi}\right)}{K_1\left(\frac{r_0}{\xi}\right)I_1\left(\frac{D_0}{\xi}\right)-I_1\left(\frac{r_0}{\xi}\right)K_1\left(\frac{D_0}{\xi}\right)}\right]\frac{r_0}{\xi} + \frac{Lr_0}{W_s\xi^2}} + R_{\text{iso}} \quad (23)$$

As evident from Eqs. (21)–(23) there can be two fitting parameters: ratios r_0/ξ_0 and L/W. These fitting parameters are not independent: According to Landau–de Gennes theory ξ_0 depends on the fundamental parameters of the system A and L, $\xi_0 = \sqrt{\frac{L}{aT^*}}$, where $a = A/(T\text{–}T^*)$. In our modeling we accepted $L = 1.7 \times 10^{-11}$ J/m, limited T^* by T_{NI} ($T^* < T_{NI}$ with $T_{NI} = 35.1$ °C), and used r_0 and ξ_0 as primary fitting parameters.

C. Results of modeling of the optical retardation vs temperature curves

We found that Eqs. (20)–(23) produce good fits in all cases; however, fitting the experimental $R_{\text{cell}}(T)$ curves does not produce a unique set of ξ_0, r_0, and T^*. Table I shows some of the combinations producing satisfactory fits. This can point toward the experimental fact that polymer networks are

TABLE II. Fitting parameters producing the minimum χ^2 fit of $R_{\text{cell}}(T)$ curves for $\xi_0 \leqslant 1$ nm.

Cell (% of RM 82)	ξ_0 (nm)	r_0 (nm)	T^*(°C)	R_{iso} (nm)
3%	0.99	2.81	305.81	9.99
3.5%	0.96	1.32	303.02	32.15
4%	0.99	0.90	304.39	13.68
5%	0.99	1.00	304.86	16.86

formed from fibrils of varying radii, which is supported by SEM data [1].

The phenomenological theories [4,15,16] limit ξ_0 by about 1 nm, and thus we performed a multiparametric minimum χ^2 fitting for $\xi_0 \leqslant 1$ nm (see Fig. 5). The results are summarized in Table II.

D. Electric-field response of the polymer-stabilized π cell in the isotropic phase

All the investigated polymer-stabilized cells have shown an unusually high birefringence in the isotropic state, even at temperatures about 70 °C above the *N-I* phase transition. This birefringence is due to the paranematic order induced by the network of fine polymer fibrils and can be used in technological applications. Thus, we performed a series of experiments on the static and dynamic response of the cells under strong electric fields at the temperatures higher than the *N-I* transition.

Figure 6 shows the optical retardation measured as a function of the temperature and of the applied voltage for the cell with the gap of $d = 5.3\,\mu$m and polymer concentration $c = 3.5\%$. As expected, R_{cell} decreases monotonically with increasing voltage. Close to the *N-I* transition, the variation of R_{cell} under the strong field is quite large, about 70 nm. With increasing temperature, the field-induced variation of R_{cell} decreases. However, its absolute value remains quite significant: It decreases to 10 nm only at $T = 70$ °C. At all

FIG. 5. Measured (symbols) and modeled (solid lines) $R_{\text{cell}}(T)$ curves for $\xi_0 \leqslant 1$ nm.
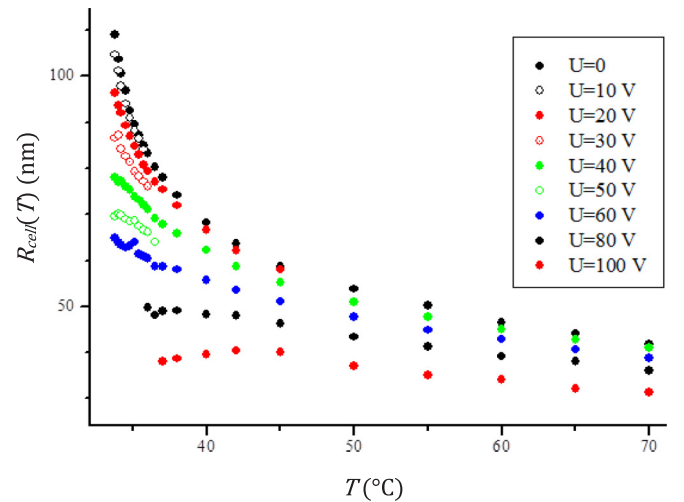
FIG. 6. $R_{\text{cell}}(T)$ curves for the cell ($d = 5.3\,\mu$m, $c = 3.5\%$) under continuously applied ac field (10 kHz; the rms values of the voltage are shown in the figure).
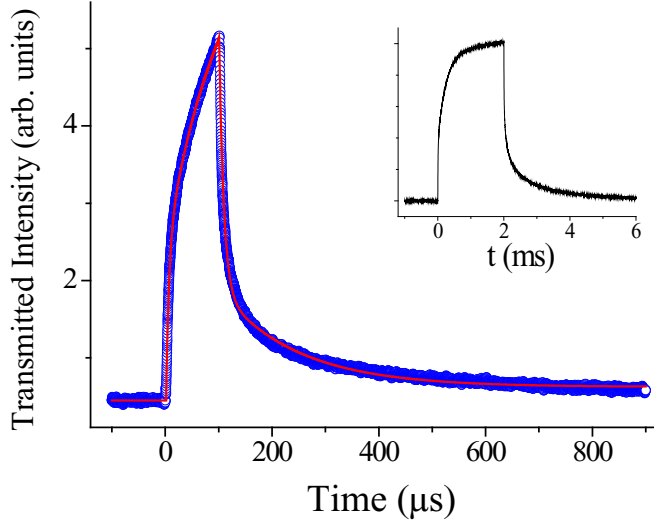
FIG. 7. Transmitted intensity of the cell ($d = 5.3\,\mu\text{m}$, $c = 3.5\%$) under crossed polarizers at $T = 36.0\,^{\circ}\text{C}$ when subjected to a short pulse of dc voltage $\tau = 100\,\mu\text{s}$, $U = 160\,\text{V}$: experiment (blue points) and fit (red lines). The red lines correspond to the fit of the on and off parts of the curve with a sum of two exponentials with characteristic times $\tau_1^{\text{on}} = 5.6\,\mu\text{s}$, $\tau_2^{\text{on}} = 110\,\mu\text{s}$, $\tau_3^{\text{off}} = 8.8\,\mu\text{s}$, and $\tau_2^{\text{off}} = 140\,\mu\text{s}$. The inset shows the response of the cell to a longer dc pulse, $\tau = 2\,\text{ms}$, revealing an additional third characteristic time, $\tau_3^{\text{on}} \approx \tau_3^{\text{off}} \geqslant 1\,\text{ms}$.

temperatures and under very strong electric fields R_{cell} decreases asymptotically toward the residual optical retardation $R_{\text{residual}} \approx 30\,\text{nm}$, i.e., the same value as R_{iso} measured at high temperatures in the absence of the external field.

Figure 7 shows the optical response of the cell with $d = 5.3\,\mu\text{m}$ and $c = 3.5\%$ at $T = 36.0\,^{\circ}\text{C}$ (in the isotropic phase) to a square pulse of 100 μs duration and amplitude of 160 V. Fitting the on and off parts of the curves with two exponents reveals two distinct and very short characteristic rise and decay times. For both shorter and longer decays the on and off times are of the same order of magnitude: $\tau_1^{\text{on}} \approx \tau_1^{\text{off}} \approx 5\,\mu\text{s}$ and $\tau_2^{\text{on}} \approx \tau_2^{\text{off}} \approx 100\,\mu\text{s}$. The transmitted light intensity significantly changes with the applied voltage and temperature; however, the characteristic times τ_1 and τ_2 remain temperature and voltage independent. Application of longer dc pulses (see inset in Fig. 7) reveals a third, longer characteristic time $\tau_3 : \tau_3^{\text{on}} \approx \tau_3^{\text{off}} \geqslant 1\,\text{ms}$, which also does not depend on temperature and applied voltage.

IV. DISCUSSION

One striking result of the present study is the very large value of the optical retardation of the cells in the isotropic phase. In fact, the observed retardation R_{cell} is at least one order of magnitude larger than the one reported in Ref. [40] for homogeneously aligned nematic cells. This large value cannot be explained solely by the bend configuration of the fibrils. Indeed, the C_ϕ value and, hence, R_{cell} is much smaller for the bend configuration of π cells than for the splay-bend configuration of the planar cells under the same voltage (in our case, 0.21 and 1, respectively).

The huge value of the observed retardation points toward the unusually large value of the average order parameter $\langle S_{\text{LC}} \rangle$ induced by the fibrils in the isotropic phase of 5CB, suggesting that the average fibril radius is very small and comparable to ξ_0, which was supported by modeling. Indeed, the modeled r_0 values obtained by using different values for the anchoring strength coefficient W range from $r_0 \approx \xi_0$ for extremely strong anchoring to $r_0 \ll \xi_0$ for weak anchoring. Also, independently of the assumptions adopted in the model, the large measured value of the LC-related retardation $R_{\text{LC}} = R_{\text{cell}} - R_{\text{residual}}$ suggests that the fibrils have a small radius. If the radius of the fibrils is small, then the surface area of the LC/polymer interface per unit volume is large. The large value of the area of the LC/polymer interface facilitates the adsorption of the LC molecules, thus inducing the paranematic ordering and increasing the bulk-average paranematic order parameter $\langle S_{\text{LC}} \rangle$, which leads to high optical retardation R_{LC}. Taking into account that at fixed polymer concentration c the surface-to-volume ratio of the polymer network is proportional to c/r_0, we conclude that for a given anchoring strength and polymer concentration the optical retardation increases with the decreasing radius of the fibrils as $1/r_0$.

The high value of the measured residual retardation R_{residual} can indicate that, in addition to the ordered polymer network, there is a significant amount of other well-oriented birefringent material that sustains its orientation at the temperatures deep in the isotropic phase. The existence of such well-oriented structure cannot be solely explained by weak and highly temperature-dependent contribution from paranematic ordering of the LC. However, if the LC molecules are absorbed on the surface of the fibrils during polymerization forming a well-oriented layer around them, then such structure can have the order parameter as high as for the nematic surrounding it: $S_{\text{LC}} = S_0 = 0.65$. Once absorbed, the LC molecules are strongly anchored by the polymer chains keeping their high degree of ordering at the temperatures far above the N-I transition temperature. In this case the absorbed nematic layer stays attached to the fibril sustaining its high and temperature-independent order parameter even at $T > T_{NI}$.

The system will then behave as if the concentration of the polymer is higher. The adsorption of LC molecules by a solid substrate is a known effect connected to the phenomenon of anchoring memory [41,42]. At the first contact with the solid substrate the mesogenic molecules are absorbed at the interface, forming a thin and oriented layer that memorizes the orientational order at the time of contact. Once memorized, the molecular order in the absorbed layer does not change because its reorientation requires energies much higher than thermal. It is subject to desorption-reabsorption effects, a very slow process called "anchoring gliding" [43]. The adsorbed layer anchors the LC molecules in the bulk serving as a new substrate. Chemical properties of the solid can facilitate the process, as happens in our case when the mesogenic monomers form fibrils that have the chemical composition similar to that of the LC.

The large electrically controlled part of the optical retardation in the isotropic state of the polymer-stabilized π cells ΔR_E makes them very attractive for technological applications. Qualitatively, three different mechanisms contribute to ΔR_E; all of them are anisotropic in nature. The electric energy

density depends on the local orientation of the LC director, which is parallel to the axes of fibrils, and the electric field, which is perpendicular to the substrates of the cell. Taking into account that the dielectric anisotropy of the LC is proportional to the order parameter, $\Delta\varepsilon = \Delta\varepsilon^0 S$ ($\Delta\varepsilon^0$ is the dielectric anisotropy when $S = 1$) the bulk energy of the nematic (apart from the term which is independent of S and ϕ and thus irrelevant to our analysis) is

$$f_{\text{bulk}} = \frac{1}{2}\left[a(T - T^*)S^2 + L\left(\frac{dS}{dr}\right)^2 - \varepsilon_0 \Delta\varepsilon^0 S E^2 \left(\sin^2\phi - \frac{1}{3}\right)\right], \qquad (24)$$

where ϕ is the tilt angle of the axis of fibrils with respect to the cell substrate.

The first effect of the electric field on such a system is the variation of the scalar order parameter S. Indeed, competition between the condensation term and the electric energy term in Eq. (24) at constant ϕ favors an increase of the scalar order parameter when $\phi > \arcsin(1/\sqrt{3})$ and its decrease in the case when $\phi < \arcsin(1/\sqrt{3})$. The same effect exists also in the nematic phase, but then it is negligibly small because of the huge condensation energy of the nematic. On the contrary, in the isotropic phase this term is important, and cannot be neglected, particularly at the temperatures close to the *N-I* transition. The variation of the order parameter is a local phenomenon, with forces transmitted only at the scale of the correlation length ξ, and thus the on and off characteristic times are expected to be in the μs range for both the nematic and isotropic phases.

The second effect of the electric field is the electric torque applied to the nematic director. If, for simplicity, one considers the case of constant S, the torque, which favors the director orientation parallel to the field, is proportional to $\sin(2\phi)$. Under this torque, the nematic director on the fibril surface and in the space between the fibrils reorients parallel to the field. The same effect is observed in pure nematics in the nematic phase; however, in the case of confinement at the scale of the interfibril distance D_0 its amplitude is small, and thus the on and off response times are expected to be short and almost equal in duration.

These two electric-field-induced effects are in fact two different aspects of the same process—the simultaneous distortion and reorientation of the LC order parameter tensor **Q**. The amplitudes and the response times of the two effects are coupled, and together these two mechanisms explain the observed fast response times, $\tau_1^{\text{on}} \approx \tau_1^{\text{off}} < 10\,\mu s$ and $\tau_2^{\text{on}} \approx \tau_2^{\text{off}} \approx 100\,\mu s$.

The slower characteristic times, $\tau_3^{\text{on}} \approx \tau_3^{\text{off}} \geqslant 1$ ms, are due to another field-induced effect: the transmission of the torque acting on the order parameter tensor **Q** to the fibrils that is due to the surface anchoring. Under this torque, the semirigid fibril is distorted at a scale comparable to its persistence length, which is significantly larger than D_0, resulting in slower response times.

It is important to note that the response times of all described effects are related to the length scale of the distortions, which is defined not by the cell thickness d, but by the structure of the polymer network and the fibrils' radii and

rigidity. Therefore, we expect that the response times will remain the same even when the cell gap is changed, allowing one to increase the field-controlled optical retardation of the cell ΔR_{E} without slowing the response times. This will require higher applied voltages, because, unlike the Fréedericksz transition [32], these effects are governed by the electric-field strength rather than voltage.

π-bend configuration in our cells is also an important factor for obtaining a large field-controlled retardation ΔR_{E}. The impact of all the three field-induced contributions to ΔR_{E} is maximum at $\phi = 45°$. Indeed, the field torque exerted on the nematic and transmitted to the fibril is proportional to $\sin(2\phi)$. This torque vanishes for both planar and homeotropic orientation of the fibril. Similarly, although the S variation is large for both $\phi = 0°$ and $90°$, the corresponding contribution to ΔR_{E} is negligible: For $\phi = 90°$, the field-induced variation of S is large, but $\Delta R_{\text{E}} = 0$ due to $C_\phi = 0$, and for $\phi = 0$, despite $C_\phi = 1$, ΔR_{E} remains small because the field-induced variation of S is very small (in this geometry the field induces only a minor biaxial distortion of the **Q**-tensor, with negligible effect on the LC birefringence). In contrast, for the π-bend geometry of the fibrils, there are large segments of the fibrils that are already tilted with respect to the field, and the amplitude of ΔR_{E} is optimized despite the moderate C_ϕ value. Thus, if the goal is to achieve the *highest* electrically controlled retardation ΔR_{E} in the isotropic phase then the π-bend structure of the fibrils is the optimal one for the same-gap cells, although the planar cell can provide a larger temperature-dependent optical retardation R_{cell}.

The optimized polymer-stabilized π cells operated in the isotropic phase are very attractive for light processing application, for example, for usage in optical switches and modulators. We have shown that the electrically controllable optical retardation of the cell operating close to the *N-I* phase transition is about 50 nm; it can be even higher for π-cells with thinner fibrils and/or larger cell gaps. The on and off response times of such cells are in the range of 10–100 μs which is two orders of magnitude faster than the relaxation times observed for the conventional nematic devices. Moreover, these times are independent of the cell gap and are expected to remain the same for thicker cells, which will provide electrically controlled optical retardation of the order of $\lambda/4$ and, therefore, an optimal contrast of the device. As an example, we present the operation of a polymer-stabilized π-cell as an optical modulator operating at the temperature 0.5 °C above the *N-I* phase transition. The cell is driven by sinusoidal ac pulses (frequency $f = 1$ kHz, voltage $U_{\text{rms}} = 40\,V_{\text{rms}}$) whereas the transmitted light is modulated at the double frequency, 2 kHz (see Fig. 8).

V. CONCLUSIONS

We developed a technique for fabrication of polymer-stabilized π cells via photopolymerization of the RM 82 monomer in the nematic 5CB under moderate electric field. The polymer network developed at these conditions consists of well-oriented fibrils that follow the π-bend director field present at the time of polymerization due to application of the external electric field. When polymerization is complete, the polymer network stabilizes the π-bend state in the nematic phase and induces a significant paranematic order in the
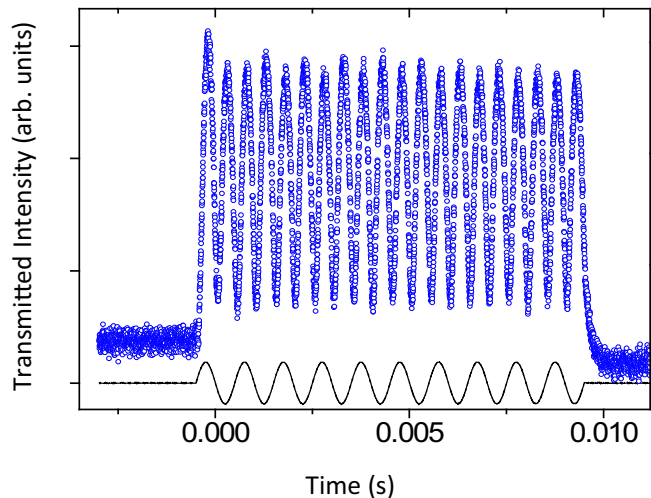
FIG. 8. Modulation of the light by a polymer-stabilized π-cell ($d = 4.3\,\mu$m, $c = 4\%$) in its isotropic state, $0.5\,°$C above the *N-I* phase transition. The cell is driven by sinusoidal ac pulses (black continuous line), with frequency $f = 1$ kHz and rms voltage $U_{\rm rms} = 40$ V. Light transmitted by the cell observed under crossed polarizers (blue data points) is modulated at the double frequency, 2 kHz.

isotropic state of the LC. By optimizing the cell thickness ($d \sim 5\,\mu$m), the monomer concentration (3–5 %) and polymerization conditions (holding voltage applied to the cell, power and wavelength of the UV light, etc.) we obtained polymer-stabilized cells with unusually high, up to 100 nm, values of the optical retardation $R_{\rm cell}$ in the isotropic phase at temperatures close to the *N-I* transition. We built a two-dimensional analytical model relating the induced paranematic order and the head-on optical retardation $R_{\rm cell}$ with the

fibrils' degree of ordering, anchoring energy, and their average radius r_0. The fit of the experimentally measured $R_{\rm cell}(T)$ curves with our theoretical model reveals that the radius of the fibrils is very small, $r_0 < 1$ nm, which leads to the high values of the head-on optical retardation for the optimized π-cells. The measured large residual retardation of the cell $R_{\rm residual}$ at the temperatures far above the *N-I* transition indicates that a thin and well-oriented layer of 5CB molecules is adsorbed on the fibrils, acting as a new, highly ordered substrate, which additionally enhances the induced paranematic order of the isotropic bulk 5CB.

We observed a strong voltage-driven decrease of the cell retardation, with the electrically controllable part of the retardation $\Delta R_{\rm E}$ being comparable to the difference $R_{\rm cell}(T) - R_{\rm residual}$ measured at the same temperature. We demonstrated that this large value of $\Delta R_{\rm E}$ is due to the π-bend geometry of the fibrils, which optimizes the coupling of the polymer-induced paranematic order with the applied electric field. The observed on and off response times of the electro-optic effect are almost the same and very fast, in the 10–100 μs range, which is at least two orders of magnitude faster than the typical relaxation times of nematic cells. Moreover, both these response times are defined only by the structure of the polymer network and are independent of the cell gap. This can allow obtaining larger $\Delta R_{\rm E}$ in thicker cells that demonstrate the same fast response times. These attractive features of the isotropic state of polymer-stabilized π-cells are promising for application in fast electro-optic devices such as optical switches and light modulators.

[1] *Liquid Crystals in Complex Geometries Formed by Polymer and Porous Networks*, edited by G. P. Crawford and S. Zumer (Taylor and Francis, London, 1996).

[2] J. W. Doane, N. S. Vaz, B. G. Wu, and S. Zumer, Field-controlled light scattering from nematic droplets, Appl. Phys. Lett. **48**, 269 (1986).

[3] K. R. Amundson and M. Srinivasarao, Liquid-crystal-anchoring transitions at surfaces created by polymerization-induced phase separation, Phys. Rev. E **58**, R1211 (1998).

[4] G. P. Crawford, A. Scharkowski, Y. K. Fung, J. W. Doane, and S. Zumer, Internal surface, orientational order, and distribution of a polymer network in a liquid crystal matrix, Phys. Rev. E **52**, R1273 (1995).

[5] K. R. Amundson, Imprinting of nematic order at polymer network surfaces as a function of cross-link density, Phys. Rev. E **59**, 1808 (1999).

[6] M. Bažec and S. Žumer, Simulation of phase separation of polymer-liquid-crystal mixtures and the effect of confining external surfaces, Phys. Rev. E **73**, 021703 (2006).

[7] M. Y. Jin, T.-H. Lee, J.-W. Jung, and J. H. Kim, Surface effects on photopolymerization induced anisotropic phase separation in liquid crystal and polymer composites, Appl. Phys. Lett. **90**, 193510 (2007).

[8] Y. Kim, J. Francl, B. Taheri, and J. West, A method for the formation of polymer walls in liquid crystal/polymer mixtures, Appl. Phys. Lett. **72**, 2253 (1998).

[9] R. Ren, S.-T. Wu, and Y.-H. Lin, *In Situ* Observation of Fringing-Field-Induced Phase Separation in a Liquid-Crystal–Monomer Mixture, Phys. Rev. Lett. **100**, 117801 (2008).

[10] D. Voloschenko, O. Pishnyak, S. Shiyanovskii, and O. Lavrentovich, Effect of director distortions on morphologies of phase separation in liquid crystals, Phys. Rev. E **65**, 060701(R) (2002).

[11] L. Lu, V. Sergan, and P. J. Bos, Mechanism of electric-field-induced segregation of additives in a liquid-crystal host, Phys. Rev. E **86**, 051706 (2012).

[12] P. Sheng, Boundary-layer phase transition in nematic liquid crystals, Phys. Rev. A **26**, 1610 (1982).

[13] K. Miyano, Wall-Induced Pretransitional Birefringence: A New Tool to Study Boundary Aligning Forces in Liquid Crystal, Phys. Rev. Lett. **43**, 51 (1979).

[14] K. Miyano, Surface-induced ordering of a liquid crystal in the isotropic phase, J. Chem. Phys. **71**, 4108 (1979).

[15] I. Amimori, J. N. Eakin, J. Qi, G. Skacej, S. Zumer, and G. P. Crawford, Surface-induced orientational order in stretched

nanoscale-size polymer dispersed liquid crystal droplets, Phys. Rev. E **71**, 031702 (2005).

[16] H. J. Coles, Laser and electric field induced birefringence studies on the cyanobiphenyl homologues, Mol. Cryst. Liq. Cryst. **49**, 67 (1978).

[17] R. E. Kraig, L. Taylor, R. Ma, and D.-K. Yang, Nematic order in polymer-stabilized liquid crystals, Phys. Rev. E **58**, 4594 (1998).

[18] S. Aya, Y. Sasaki, F. Araoka, K. Ishikawa, K. Ema, and H. Takezoe, Isotropic-nematic transition at the surface of a liquid crystal embedded in an aerosil network, Phys. Rev. E **83**, 061714 (2011)].

[19] P. A. Lebwohl and G. Lasher, Nematic-liquid-crystal order—a Monte Carlo calculation, Phys. Rev. A **6**, 426 (1972).

[20] C. Chiccoli, P. Pasini, G. Skacej, C. Zannoni, and S. Zumer, Polymer network-induced ordering in a nematogenic liquid: A Monte Carlo study, Phys. Rev. E **65**, 051703 (2002).

[21] U. Fabbri and C. Zannoni, A Monte Carlo investigation of the Lebwohl-Lasher lattice model in the vicinity of its orientational phase transition, Mol. Phys. **58**, 763 (1986).

[22] A. V. Koval'chuk, M. V. Kurik, O. D. Lavrentovich, and V. V. Sergan, Electrooptical effects in the polymer dispersed liquid crystals: Response time, Mol. Cryst. Liq. Cryst. **193**, 217 (1990).

[23] V. G. Nazarenko, Yu. A. Reznikov, V. Yu. Reshetnyak, V. V. Sergan, and V. Ya. Zyryanov, Oriented dispersion of liquid crystal droplets in a polymer matrix with light induced anisotropy, Mol. Mater. **2**, 295 (1993).

[24] V. Sergan, X. Wang, P. J. Bos, and G. D. Sharp, Fast switching polymer stabilized splay cell, Mol. Cryst. Liq. Cryst. **410**, 487 (2004).

[25] T. Sergan, V. Sergan, and B. MacNaughton, High-performance active liquid crystalline shutters for stereo computer graphics and other 3-D technologies, J. Disp. Technol. **3**, 29 (2007).

[26] B. G. Wall and J. L. Koenig, Studying the curing kinetics of a diacrylate by using infrared spectroscopy, Appl. Spectrosc. **51**, 1453 (1997).

[27] L. Lu, T. Sergan, V. Sergan, and P. J. Bos, Spatial and orientational control of liquid crystal alignment using a surface localized polymer layer, Appl. Phys. Lett. **101**, 251912 (2012).

[28] P. Bos, V. Sergan, and T. Sergan, Photo-patterned pre-tilt liquid crystal cells, lenses, and methods, US Patent No. 0,170,039 A1, 2011.

[29] V. Sergan, T. Sergan, and P. Bos, Control of the molecular pretilt angle in liquid crystal devices by using a low density localized polymer network, Chem. Phys. Lett. **486**, 123 (2010).

[30] T. Sergan, V. Sergan, R. Herrera, L. Lu, P. J. Bos, and E. Sergan, In-situ control of surface molecular order in liquid crystals using a localized polymer network and its application to electro-optical devices, Liq. Cryst. **40**, 72 (2013).

[31] T. Sergan, I. Dozov, V. Sergan, and R. Voss, Comparative study of the anchoring strength of reactive mesogens and industrial polyimides used for the alignment of liquid crystals, Phys. Rev. E **95**, 052706 (2017).

[32] G. Barbero and L. R. Evangelista, *Absorption Phenomena and Anchoring Energy in Nematic Liquid Crystals* (Taylor and Francis, London, 2006).

[33] M. Nobili and J. Durand, Disorientation-induced disordering at a nematic-liquid crystal-solid interface, Phys. Rev. A **46**, R6174 (1992).

[34] M. Abramovwitz and I. Stegun, *Handbook of Mathematical Functions* (McGraw-Hill Book Company, New York, 1964).

[35] I. S. Gradsteyn, I. M. Ryzhik, A. Jeffrey, and D. Zwillinger, *Table of Integrals, Series and Products* (Academic Press, New York, 2000).

[36] Yu. Nastishin, R. D. Pollak, S. V. Shiyanovskii, and O. D. Lavrentovich, Determination of nematic polar anchoring from retardation versus voltage measurements, Appl. Phys. Lett. **75**, 202 (1999).

[37] Yu. Nastishin, R. D. Pollak, S. V. Shiyanovskii, V. H. Bodnar, and O. D. Lavrentovich, Nematic polar anchoring strength measured by electric field technique, J. Appl. Phys. **86**, 4199 (1999).

[38] K. Y. Han, T. Miyashita, and T. Uchida, Accurate measurement of the pretilt angle in a liquid crystal cell by an improved crystal rotation method, Mol. Cryst. Liq. Cryst. **241**, 147 (1994).

[39] TWIST CELL OPTICS 7.2 software developed at Liquid Crystal Institute, Kent State University, Kent, OH, USA, 2002.

[40] J.-H. Kim, R. G. Petschek, and C. Rosenblatt, Electro-optic response of surface induced nematic order above the nematic-isotropic phase transition temperature, Phys. Rev. E **60**, 5600 (1999).

[41] I. Dozov, D. N. Stoenescu, S. Lamarque-Forget, P. Martinot-Lagarde, and E. Polossat, Planar degenerated anchoring of liquid crystals obtained by surface memory passivation, Appl. Phys. Lett. **77**, 4124 (2000).

[42] S. Joly, K. Antonova, P. Martinot-Lagarde, and I. Dozov, Zenithal gliding of the easy axis of a nematic liquid crystal, Phys. Rev. E **70**, 050701 (2004).

[43] D. N. Stoenescu, I. Dozov, and P. Martinot-Lagarde, Long-time behavior of the azimuthal anchoring strength and easy axis gliding of nematic liquid crystal, Mol. Cryst. Liq. Cryst. **351**, 427 (2000).